QUICKLOOK GRAVITY FIELD SOLUTIONS AS PART OF THE GOCE QUALITY ASSESSMENT

Reinhard Mayrhofer[(1)], Roland Pail[(2)], Thomas Fecher[(2)]

[(1)] Graz University of Technology, Institute of Navigation and Satellite Geodesy, Steyrergasse 30, 8010 Graz, Email: reinhard.mayrhofer@tugraz.at
[(2)] Technical University Munich, Institute of Astronomical and Physical Geodesy, Arcisstraße 21, 80333 Munich, Email: pail@bv.tum.de

ABSTRACT

The Quick-Look Gravity Field Analysis (QL-GFA) is a component of the Routine & Rapid Processing Facilities in the framework of the ESA-funded project "GOCE High-level Processing Facility", an operational hardware and software system for the scientific processing of GOCE data, in order to derive a spherical harmonic Earth's gravity field model from the GOCE orbits based on satellite-to-satellite tracking (SST) in high-low mode, and satellite gravity gradiometry (SGG) data with very short latencies. Thus with the QL-GFA it is possible to monitor the quality of the input data and to derive a fast diagnosis of the GOCE system performance on gravity field model level. The QL-GFA is based on a semi-analytic approach, applying Fast Fourier Transform techniques to derive gravity field models within a few hours of computation time. Key products are gravity field models as SGG-only, SST-only, and combined solutions, as well as estimates of the gradiometer error power spectral density computed from the residuals of a SGG-only gravity field analysis.

1. INTRODUCTION

The scientific GOCE data processing (Level 1b to Level 2) is performed by the "European GOCE Gravity Consortium" (EGG-C), a consortium of 10 European university and research institutes, in the framework of the ESA-funded project "GOCE High-Level Processing Facility" ([16]). In addition to the production of precise GOCE orbits, calibrated gravity gradients and a high-accuracy, high-resolution GOCE spherical harmonic model of the Earth's gravity field including variance-covariance information (in a post-processing step), one component of HPF deals with the generation of quick-look products (rapid science orbits, approximate gravity field models) already in parallel to the GOCE measurement phases. The main purpose of these quick-look products is to derive a fast diagnosis of the GOCE sensor systems, and thus to contribute to ESA's calibration and validation activities. In the frame of this HPF contract, the "Sub-processing Facility (SPF) 6000", a co-operation of TU Graz, Austrian Academy of Sciences, University of Bonn, and TU Munich, under the lead of TU Graz, is – in addition to the production of a high-precision GOCE gravity field model – also responsible for the processing of quick-look gravity field models from preliminary GOCE orbit data applying satellite-to-satellite tracking in the high-low mode (hl-SST), and satellite gravity gradiometry (SGG), cf. [8].

2. KEY TASKS OF QL-GFA

Key tasks of QL-GFA are:

- Check of SGG and hl-SST input data in parallel to the mission and analysis of partial / incomplete SGG and hl-SST data sets.
- Computation of quick-look gravity field models (SST-only, SGG-only, combined SST+SGG) for the purpose of a fast analysis of the information content of the input data on the level of the gravity field solution.
- Delivery of near real-time gravity field solutions (QL-A) and high resolution gravity field models with short latencies of below 4 days (QL-B).
- Estimation of the gradiometer error PSD (power spectral density) from the residuals of a SGG-only gravity field analysis.
- Quality analysis: Hypothesis testing of derived coefficient solutions and statistical error estimates against prior models.
- Production of Quality Report Sheets.

QL-GFA is applied at two stages: Quick-Look-A (QL-A) is applied to Level 1b preliminary orbits (SST_POS_2C, accuracy ~10 m) and the Level 1b gravity gradients (EGG_GGT_2C). The main purpose at this stage is a rough check of the SGG measurement time series, with special emphasis on the evaluation of the SGG error PSD. For QL-A, consecutive gravity field solutions are available in a daily interval. They are generated with a latency of 4 hours after arrival of all required input data.

Quick-Look-B (QL-B) is applied after the availability of the Level 2 rapid science orbit solution (accuracy in the decimetre range, SST_RSO_2) and the calibrated gravity gradients (EGG_NOM_2I). For QL-B, consecutive gravity field solutions are available in a

Proc. 'ESA Living Planet Symposium', Bergen, Norway
28 June – 2 July 2010 (ESA SP-686, December 2010)

weekly interval. The maximum degree and order for the QL-GFA gravity field models are optimized with respect to the global coverage of the input data, and are now in the range between degree/order 160 to 185. Additionally to the regular processing of weekly solutions, also a high resolution gravity field model has been computed from two months of cycle-1 (November/December 2009) data with a resolution of degree/order 200.

3. FUNCTIONAL MODEL

The QL-GFA is based on the semi-analytic approach. While in the direct, time-wise and space-wise solution strategies ([2], [8], and [7], respectively), the observations are regarded as functions of the geographical location (r,ϑ,λ), they can also be considered as a periodic time-series for one repeat period ([15]). Assuming a circular orbit, the gravitational potential V and also derived gravity functionals $V^{(\kappa)}$ can be rewritten as a Fourier series

$$V^{(\kappa)}(t) = \sum_m \sum_k \left[A_{km}^{(\kappa)} \cos\psi_{km}(t) + B_{km}^{(\kappa)} \sin\psi_{km}(t) \right] \quad (1)$$

where $\psi_{km}(t)$ is related to the two fundamental frequencies ω_o (satellite orbit revolution) and ω_e (Earth's rotation). The spherical harmonic coefficients C_{lm}, S_{lm} of the same order m are lumped together in a linear way to compose the Fourier coefficients $A_{lm}^{(\kappa)}$ and $B_{lm}^{(\kappa)}$ ([15]), leading to a block-diagonal structure of the corresponding normal equation matrix. More details on the QL-GFA functional model and software strategy can be found in [10], [11], [12] and [13].

QL-GFA solutions complete to degree/order 250 can be processed within one to two hours on a standard PC. The efficiency and speed of QL-GFA is founded mainly on the application of FFT techniques, a simplified filter strategy in the spectral domain to cope with the coloured noise characteristics of the gradiometer, and the assumption of block-diagonality of the normal equation matrix. Deviations from this assumption are incorporated by means of an iterative procedure.

A detailed discussion of the theory and the mathematical models of the QL-GFA software can be found in [9].

4. SOFTWARE ARCHITECTURE

Fig. 1 shows the architectural design, the main components and the product flow through the QL-GFA software system.

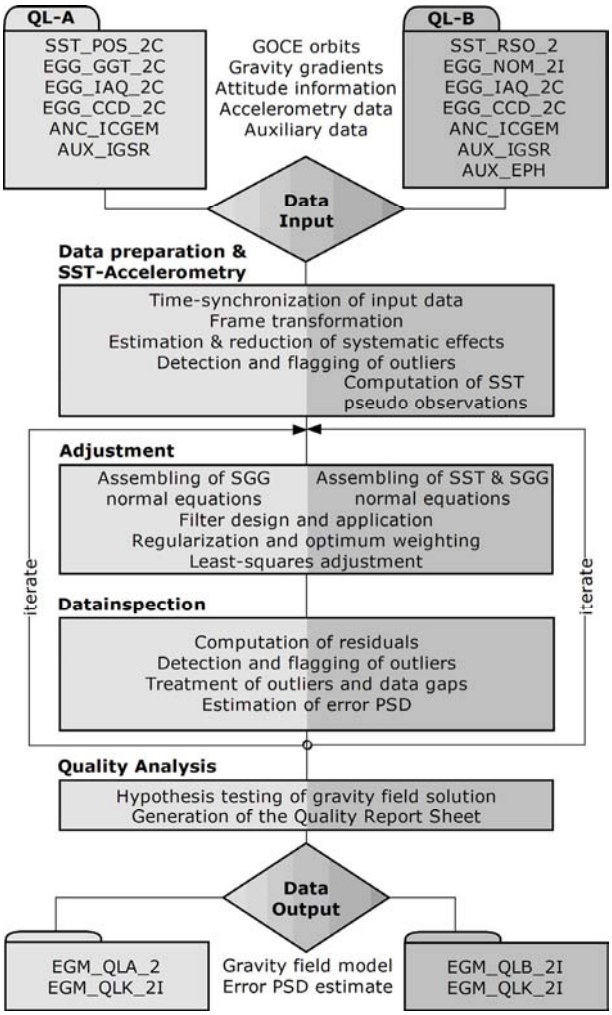

Figure 1. QL-GFA: Architectural design and product flow

In the following, the main modules shall be briefly described.

Input:
In the case of QL-A processing, exclusively Level 1b data and several auxiliary data products are used. In this software mode, the start of the processing is fully automated. It is checked in regular intervals whether new data have arrived via the official HPF interface, the processing is started and operated automatedly until the delivery of the QL-GFA output products again via the official interface.
In the case of QL-B processing, Level 1b data (e.g., attitude information, accelerometry data), Level 2 data (rapid science orbits, preliminary externally calibrated gradients), and auxiliary products are used.

Data Preparation and SST-Accelerometry:
During this pre-processing phase, orbit and gradiometry data are time-synchronized, and the transformation among different reference frames (gradiometer

reference frame (GRF), inertial frame, Earth-fixed frame) is computed. Potentially occurring systematic and extreme long-periodic effects in the SGG measurement time series are estimated and reduced, and outlier detection strategies are applied to the input time series. The SST processing is based on the energy integral approach ([1], [3]). Therefore, in the case of the processing of SST-only or combined SST+SGG solutions, the SST pseudo-observations are computed, including the correct treatment of non-conservative forces and tidal effects.

Adjustment:
The normal equations are assembled applying the functional model described in chapter 3. As filter information, representing the metrics of the system, either an a-priori noise model, or alternatively the error PSD estimates derived in the previous iteration are used. The normal equation systems are superposed, applying optimum weights for the individual SGG components V_{XX}, V_{YY} and V_{ZZ}, and the SST component. These weights are derived by variance-component estimation ([5]). Finally, the coefficients are computed by a block-wise least squares adjustment, where, optionally, spherical cap regularization ([6]) is applied to near-zonal coefficients in order to stabilize the solution in the polar gap regions.

Data Inspection:
The residuals related to the coefficient estimates are computed and checked for outliers. Based on the cleaned SGG residuals, the gradiometer error PSD is estimated, which can be used as filter information in the subsequent iteration.

Table 1. Output products of QL-GFA

Identifier	Product description
EGM_QLA_2	QL gravity field solution from SGG-only, based on Level 1b data
EGM_QLB_2I EGM_QST_2I EGM_QSG_2I EGM_QCO_2I EGM_QQR_2I	QL solutions based on Level 2 data: SST-only gravity field model SGG-only gravity field model combined SST+SGG grav. model Quality Report Sheet
EGM_QLK_2I	GOCE error PSD estimate

Output:
Tab. 1 gives an overview of the official output products. Additionally, several internal products (residuals, flags, regularization and weighting parameters) are generated.

These products are also used as prior information for the Core Solver processing, i.e., the processing of a high-accuracy GOCE Earth's gravity field model and the corresponding full variance-covariance matrix, which is the second main task of SPF 6000 ([10]).

5. QL-A OPERATIONAL PHASE RESULTS

As mentioned in chapter 2, QL-A is applied to Level 1b preliminary orbits (with an accuracy in the order of 10 to 20 m), and to Level 1b gravity gradients. Main output products are a SGG-only gravity field solution, and a first estimate of the SGG error PSDs, complemented by a quality report. The start of the processing and the operation are fully automated.

The operational QL-A processing has been started after being twenty-one consecutive days of SGG and SST data being available, which was on 18th February 2010. The complete automated process has been initiated on 15th April 2010. Because of occurring data gaps ([4], [14]) and oscillations within the analysis period, the data input window has been optimized between twenty-one and twenty-eight days. Thus, the computed solutions were applied on at least nineteen days of available data. Correspondingly, the maximum degree of resolution has been changed depending on the length of available data sets. While in the first two months a spatial resolution of degree/order 160 has been chosen, it has been increased to 170 since end of June.

Since April 2010 eighty QL-A gravity field models have been delivered to the HPF Central Processing Facility (CPF). The processing time for a QL-A SGG-only solution up to degree/order 160 is about one hour on a standard PC for fifteen iterations. Thus, together with the time consumption for quality assessment and the automated production of the quality report, the latency requirement of 4 hours can be easily met.

One of the key tasks of the QL-A processing is to identify potentially occurring data problems or inconsistencies, only Kalman-Filter re-initialization issues (which result from seldomly occurring problems in the Level 1b data processing when combining gravity gradient and star-tracker observations for attitude reconstruction), which prevented the algorithm to converge, have been removed manually from the data sets. Beam-outs and other short-term events have been left in the data for being able to see their influence on gravity field model level.

The first main product of the QL-A chain (EGM_QLA_2) contains the spherical harmonic coefficients of the SGG-only solution, as well as a gravity field report. Fig. 2 shows the coefficients deviation between a QL-A solution for cycle-1 and EGM2008 (upper) and its standard deviation (lower).
In general the QL-A gravity models are consistent to the EGM2008 model. The coefficient plot shows that there are groups of coefficients (stripes at d/o 16, 32 and 48) which can be estimated only with lower accuracy. This effect is due to the fact that there are prominent peaks in the gradiometer error PSD at frequencies which are

multiples of the satellite's revolution. Since the coefficients of d/o 16, 32, 48, etc. are sensitive to these frequencies, the degraded measurement accuracy at these specific frequencies is directly mapped into the gravity field recovery. As expected, below d/o 40 the SGG-only solution performs worse than for higher degrees/orders. As there is only a very weak spherical cap regularization ([6]) applied, the zonal and near-zonal coefficients perform worst.

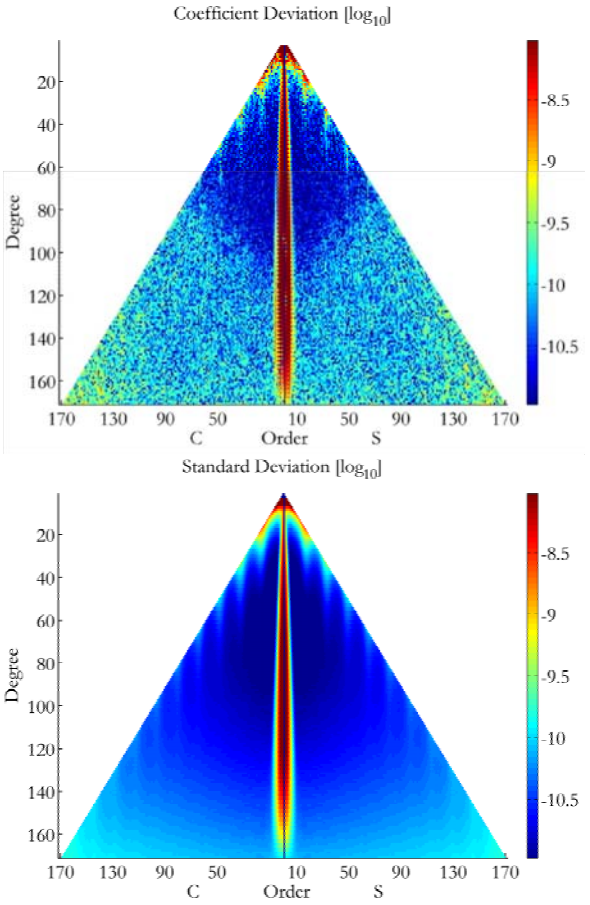

Fig. 2. QL-A cycle-1 coefficients deviation to EGM2008 (upper) and its standard deviation (lower) scaled between 10^{-11} and 10^{-8} and d/o 0 to 170.

In the frame of the gravity field adjustment, the residuals can be derived as the difference between the adjusted and the measured gradients. In the case of the consistency of the stochastic modeling, these residuals are an estimate of the observation error. The spectral representation of these residuals, as shown in terms of estimated error PSDs presented in Fig. 3, illustrate that there is still signal information in the residuals.. The peak at $3 \cdot 10^{-2}$ Hz visible best for V_{xx} (blue) is a result of spectral leakage, i.e., high-frequency signals in the gradients which can not be represented by a parameterization limited to degree/order 160.

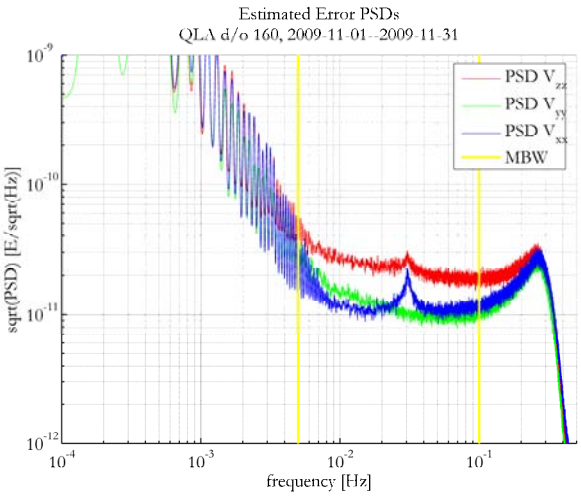

Figure 3. QL-A estimated error PSDs based on one month of cycle-1 data.

Moreover the V_{xx} (blue) component behave nearly white within the measurement bandwidth (MBW, yellow), while V_{yy} (green) is not. The V_{zz} performs substantially worse that the other two main diagonal component. Compared to the original gradiometer specification, overall the gradiometer performance is degraded by a factor of about 2.

6. QL-B OPERATIONAL PHASE RESULTS

The QL-B processing chain was initiated March 23th 2010. Although 28 days of continuous data was not available at this time, the computation of a QL-B gravity field solution was made possible by extensive manual pre-processing. Kalman-filter re-initializations, data inconsistencies and Beam-outs were removed from the data. In May 2010 the regular QL-B processing was started. Three gravity field models (SGG-only, SST-only and combined) and corresponding auxiliary products (PSDs, quality report sheets) were computed and delivered every week with not more than two days of latency. Although the QL-B processing incorporates manual pre-processing for optimal results, this latency is well within the requirements.
In the QL-B operation mode, QL-GFA is applied to Level 2 reduced-dynamic rapid science orbits (with an accuracy in the decimetre range) and Level 2 preliminary calibrated gravity gradients.

QL-B solutions (EGM_QLB_2I) are processed for the configurations:

- SST-only (EGM_QST_2I)
- SGG-only (EGM_QSG_2I)
- Combined solution (EGM_QCO_2I)

The coloured lines in Fig. 4 show the gravity field solution in terms of the degree error median

$$\sigma_l = median_m \left\{ \left| \overline{R}_{lm}^{(est)} - \overline{R}_{lm}^{(EGM)} \right| \right\} \qquad (2)$$

where $\overline{R}_{lm} = \left\{ \overline{C}_{lm}; \overline{S}_{lm} \right\}$ are the fully normalized spherical harmonic coefficients, *(est)* denotes the estimated quantities, and *(EGM)* refers to the reference model EGM2008.

The results of the three QL-B solutions (SST-only, SGG-only and combined) in terms of the degree error median for the cycle-1 (Nov. 2009 – Dec. 2009) are presented in Fig. 4. The combined SST+SGG solution (dark blue) is stabilized at low-degree range mainly by the SST component (yellow), and dominated by SGG (light blue) from about degree 80 onwards.

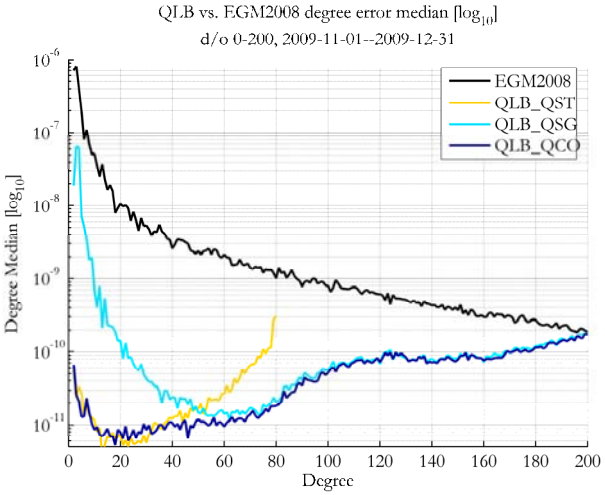

Figure 4. QL-B cycle-1 degree error median, EGM2008.

The rather high cross-over degree is related to the fact that reduced-dynamic orbits, which include GRACE prior information, are used for the quick-look processing. Thus, its performance w.r.t. EGM2008 and EIGEN-5C is extremely good at low degrees/orders (0-80). For higher degrees/orders it can be seen that the benefit of GOCE comes in. The good performance of GOCE high degrees/orders adds new gravity field information and is able to improve existing models.

In Fig. 5 the estimated error PSDs for the QL-B SGG components of the cycle-1 solution (up to d/o 200) are presented. It can be seen that the V_{zz} error PSD (red) is, compared to V_{xx} and V_{yy}, worse at lower frequencies and not white within the MBW (yellow). Also the estimated error PSD of the V_{yy} component performs worse at lower frequencies and is not completely white within the MBW.

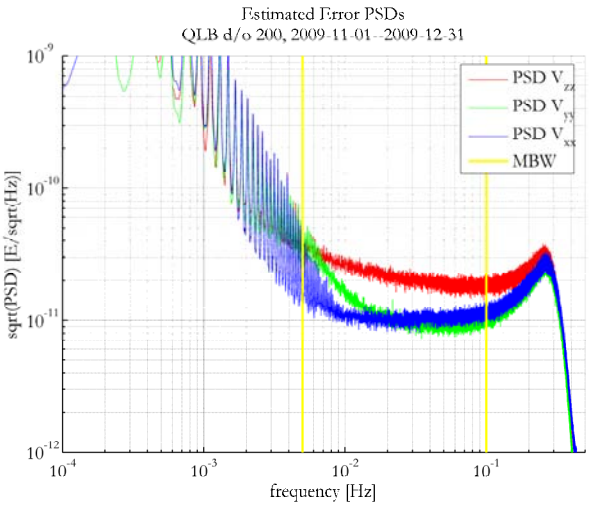

Figure 5. QL-B estimated error PSDs cycle-1.

Fig. 6 shows the coefficient deviations between the cycle-1 QL-B combined gravity field model, and EGM2008 (upper) and their standard deviation (lower).

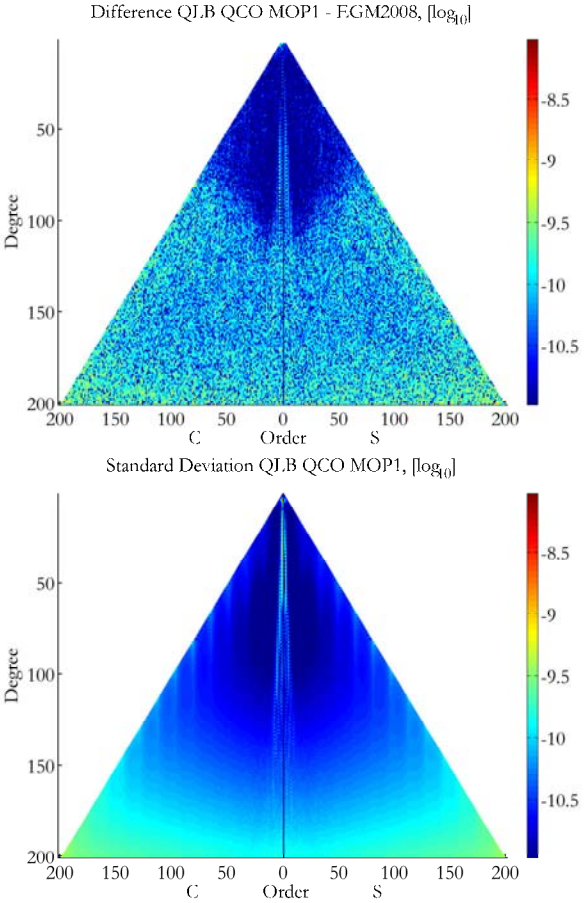

Figure 6. QL-B coefficient deviation to EGM2008 (upper) and corresponding standard deviation (lower) in logarithmic scale.

For degree/order 0 to 100 the coefficient standard deviation shown in Fig. 6 (lower) fits very well to the coefficient deviation to EGM2008, which states that the dynamic orbits reproduce the long wave GRACE information. For higher degrees/orders the standard deviations are smaller than the residuals to EGM2008. Thus, for high degrees/orders GOCE gravity field models contribute new information. Fig. 7, which shows the cumulative geoid height deviation between the combined QL-B cycle-1 solution and EGM2008 (upper) and EIGEN-5C (lower), underlines this statement. It can be seen that at regions where no or bad terrestrial data are available (Amazonas, Antarctica, Himalaya, Africa) new gravity field information is added.

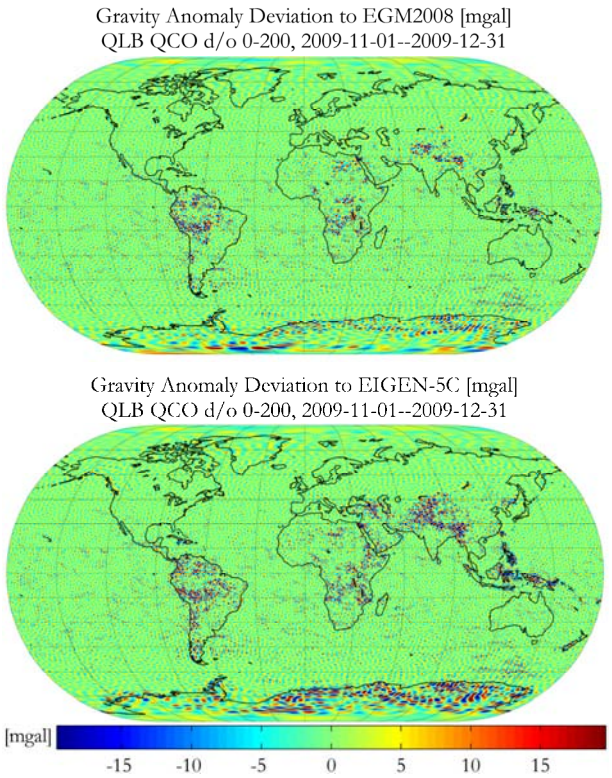

Figure 7. QL-B combined solution cumulative gravity anomaly deviations to EGM2008 (upper) and EIGEN-5C (lower) for degree/order 0 to 200

7. QL-A vs. QL-B SGG-ONLY

As already mentioned in chapter 5 an 6, while the QL-A chain is completely automated, in the QL-B processing some manual data pre-processing is incorporated. Moreover, while the QL-A chain uses level 1b products (SST_POS_2C and EGG_GGT_2C), QL-B incorporates both level 1b and level 2 data (SST_RSO_2 and EGG_NOM_2I).

As the quality of the SGG-only solutions mainly depends on the gradiometry performance, the QL-A and the QL-B SGG-only models should deliver comparable results for identical data sets. Fig. 8 shows the degree error median of such two QL-A and QL-B gravity field models based on the data from cycle-1 (November - December 2009). It can be seen that their differences are very small.

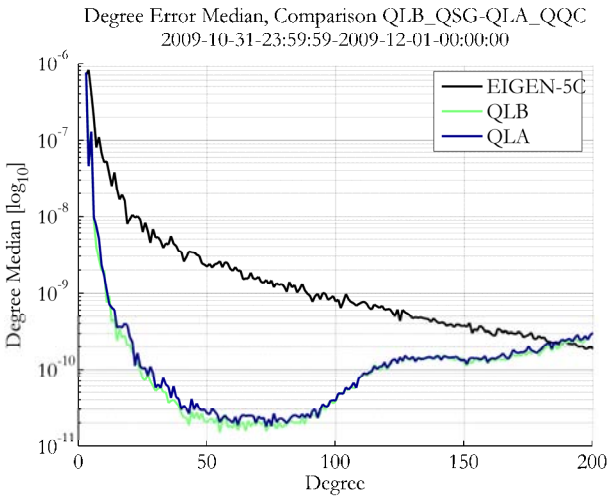

Figure 8. Degree error median of a cycle-1 QL-A and QL-B SGG-only solution compared to EIGEN-5C.

The differences seen in Fig. 8 is a result of different data pre-processing and the type of input orbits used. While the QL-B chain uses reduced-dynamic orbits (SST_RRD_2 being a sub-product of SST_RSO_2) with very few data gaps, the QL-A automated processing incorporates orbit positions based on raw GPS-data (SST_POS_2C). These orbits show many gaps especially near the poles, which causes the overall geometrical redundancy to be reduced.

8. QL-B vs. CORE SOLVER

As already mentioned in chapter 6, beside the weekly QL-B gravity field models, a cycle-1 QL-B solution has been computed with maximal degree/order 200. This QL-B gravity field model can be used for a general test of consistency by comparing it with the WP 6000 Core Solver gravity field model ([8]). The degree error median presented in Fig. 9 shows that the models are consistent to each other.

The black line in Fig. 9 represents the degree median of the core solver model, while the blue one is the degree difference median computed from the Core Solver and the QL-B coefficients. For degrees/orders lower than 60 the deviation between both models becomes larger. This is because the QL-B SST part is based on the reduced-dynamic orbit, which mainly reproduces GRACE, while the Core Solver SST part uses the kinematic orbit, which is not constrained towards an a-priori gravity field model. For medium frequency degrees/orders both models are relatively similar, but at higher degrees/orders the deviation becomes larger.

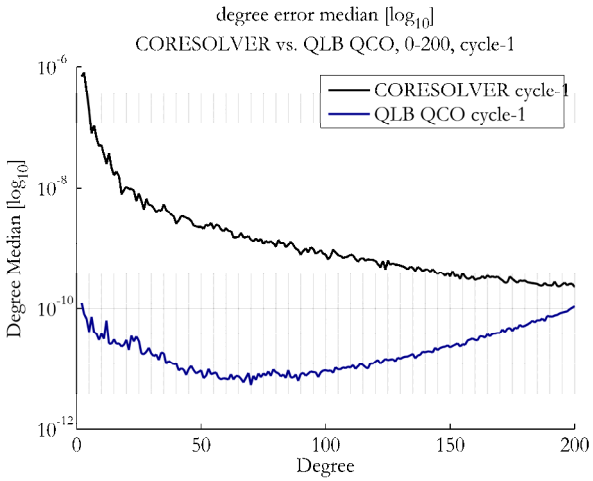

Fig. 9. Degree error median of a cycle-1 QL-B combined solution compared to the Core Solver cycle-1 gravity field model.

The QL-B processing chain has been designed for delivering fast results at the cost of precision at shorter wavelengths. Thus, the overall performance of the combined QL-B model is slightly worse than the Core Solver solution. Also the coefficient differences show that the QL-B processing performs well up to degree/order 200. In Fig. 10 it can be seen that the overall difference is below 10^{-10} up to degree/order 170, while the QL-B becomes worse at higher frequencies. Also the different regularization is visible at zonal and near zonal coefficients.

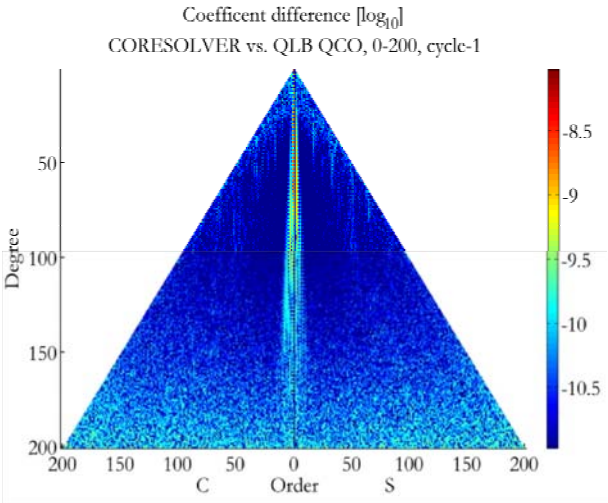

Figure 10. Coefficients difference of a cycle-1 QL-B combined solution and the Core Solver cycle-1 gravity field model

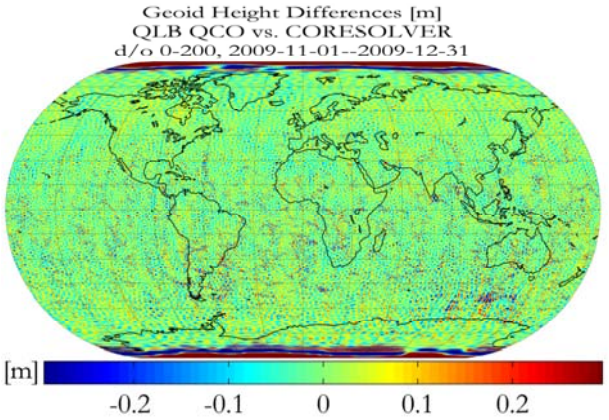

Figure 11. Cumulative geoid height differences of a cycle-1 QL-B combined solution compared to the Core Solver cycle-1 gravity field model

In Fig. 11 the cumulative Geoid height difference between the Core Solver and the cycle-1 QL-B solution is presented. It can be seen that the overall difference is homogeneous, except for Polar Regions, where the different input orbits and regularization comes in. There are deviations visible south of Australia. These are caused by some spurious tracks of the gradient component V_{yy}, which did not perform like expected. For both, the QL-B and Core Solver solution they have not been removed, but in the QL-B processing the relative data weighting worked differently, which explains the difference.

9. SUMMARY AND CONCLUSIONS

In this paper the architectural design of the Quick-Look Gravity Field Analysis software as part of the Sub-Processing Facility 6000, and its performance within the operational phase is described. The software is performing well and works continuously. Due to the fact that the semi-analytic approach, underlying QL-GFA, is based on several simplifying assumptions, compared to the Core Solver solution the accuracy of the gravity field products is slightly decreased. However, the system specification that the QL solution shall not perform worse by a factor of 10 than the high-precision solution is met with ease. Most important, the main goal, i.e. to perform a check of the input data on the level of a gravity field solution, is achieved. Fig. 12 shows the cumulative geoid heights (upper) and gravity anomalies for the cycle-1 QL-B combined solution.

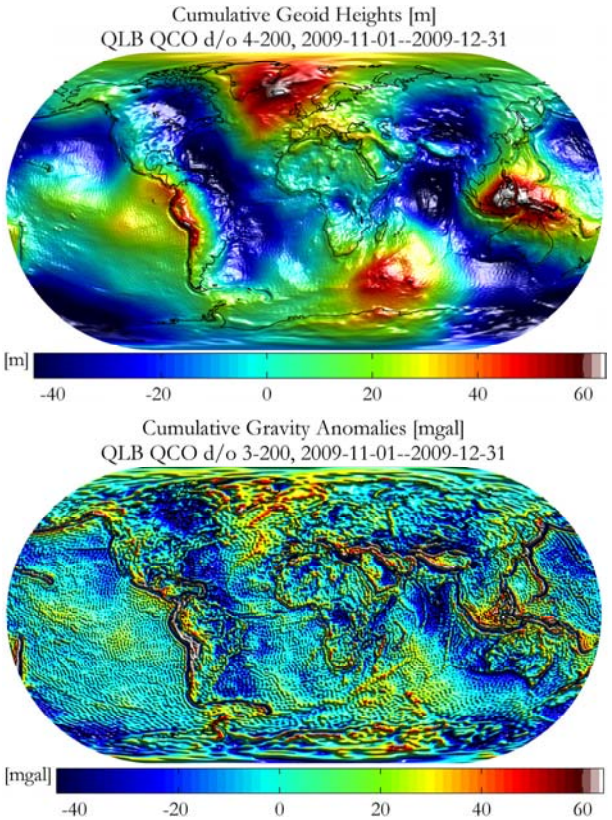

Figure 12. Cumulative geoid heights (upper) and gravity anomalies (lower) of the QL-B cycle-1 combined SGG+SST gravity field model d/o 4-200.

10. ABBREVATIONS

CPF	Central Processing Facility
EGG-C	European GOCE Gravity Consortium
FFT	Fast Fourier Transformation
GOCE	Gravity and steady-state Ocean Circulation Explorer
GRACE	Gravity Recovery and Climate Experiment
HPF	High-level Processing Facility
PSD	Power Spectral Density
QL-GFA	Quicklook Gravity Field Analysis
SGG	Satellite Gravity Gradients
SPF	Sub-Processing Facility
SST	Satellite-to-Satellite Tracking
WP	Work Package

11. REFERENCES

1. Badura, T., et al. (2006). Derivation of the CHAMP-only global gravity field model TUG-CHAMP04 applying the energy integral approach. *Stud. geophys. geod.*, 50, 59 – 74.
2. Bruinsma, S., Marty, J.C. & Balmino, G. (2004). Numerical simulation of the gravity field recovery from GOCE mission data. In: Proc. of 2nd International GOCE User Workshop. Frascati, Italy, March 8-10, 2004.
3. Földvary, L., et al. (2004) Gravity Model TUM-2Sp Based on the Energy Balance Approach and Kinematic CHAMP Orbits. In: Reigber et al. (eds.), *Earth Observation with CHAMP - Results from Three Years in Orbit*, 13-18, Springer Verlag.
4. Kern, M., et al. (2005). Outlier detection algorithms and their performance in GOCE gravity field processing. *J. Geod.*, 78, 509–519.
5. Koch, K.-R. & Kusche, J. (2002). Regularization of geopotential determination from satellite data by variance components. *J. Geod.*, 76, 259-268.
6. Metzler, B. & Pail, R. (2005). GOCE data processing: the Spherical Cap Regularization Approach. *Stud. Geophys. Geod.*, 49, 441-462.
7. Migliaccio, F. et al. (2003). Spacewise approach to satellite gravity field determinations in the presence of coloured noise. J. Geod, 78, 304 - 313.
8. Pail, R., Goiginger, H. Mayrhofer, R., Schuh, W.-D., Brockmann, J.M, Krasbutter, I., Höck, E., Fecher, T. (2010). GOCE gravity field model derived from orbit and gradiometry data applying the time-wise method. Proceedings of the ESA Living Planet Symposium, 28 June – 2 July 2010, Bergen, Norway.
9. Pail, R., et al. (2003). *Quick-Look Gravity Field Analysis (QL-GFA)*. DAPC Graz, Phase Ia, Final Report, WP Ia-4.1, 107 - 161, Graz.
10. Pail, R., et al. (2006). GOCE gravity field analysis in the framework of HPF : operational software system and simulation results. *Proc. 3rd GOCE User Workshop*, Frascati, November 2006, European Space Agency, Noordwijk.
11. Pail, R. & Plank, G. (2002). Assessment of three numerical solution strategies for gravity field recovery from GOCE satellite gravity gradiometry implemented on a parallel platform. *J. Geod.*, 76, 462 – 474.
12. Pail, R. & Plank, G. (2004). GOCE Gravity Field Processing Strategy. *Stud. Geophys. Geod.*, 48, 289-308.
13. Pail, R. & Wermuth, M. (2003). GOCE SGG and SST quick-look gravity field analysis. *Advances in Geosciences*, 1, 5 – 9.
14. Preimesberger, T. & Pail R. (2003). GOCE quick-look gravity solution: application of the semianalytic approach in the case of data gaps and non-repeat orbits. *Studia geoph. et geod.*, 47, 435 – 453.
15. Rummel, R., et al. (1993). Spherical harmonic analysis of satellite gradiometry. *Neth. Geod. Comm., Publications on Geodesy*, 39, Delft, The Netherlands
16. Rummel R, et al. (2004). High Level Processing Facility for GOCE: Products and Processing Strategy. *Proc. of the 2nd Internat. GOCE User Workshop*, Frascati.